ACS OMEGA

http://pubs.acs.org/journal/acsodf

Article

Inhibition Effect and Molecular Mechanisms of Quercetin on the Aβ42 Dimer: A Molecular Dynamics Simulation Study

Mei Fang,* Xin Wang, Kehe Su, Xingang Jia, Ping Guan,* and Xiaoling Hu*

Cite This: *ACS Omega* 2023, 8, 18009−18018

Read Online

ACCESS | Metrics & More | Article Recommendations | Supporting Information

ABSTRACT: Amyloid-β (Aβ) dimer as the smallest oligomer has recently been drawing attention due to its neurotoxicity, transient nature, and heterogeneity. The inhibition of Aβ dimer's aggregation is the key to primary intervention of Alzheimer's disease. Previous experimental studies have reported that quercetin, the widespread polyphenolic constituent of multiple fruits and vegetables, can hamper the formation of Aβ protofibrils and disaggregate Aβ fibrils. However, the molecular mechanisms of quercetin in the suppression of the Aβ(1−42) dimer's conformational changes still remain elusive. In this work, to investigate the inhibitory mechanisms of quercetin molecules on the Aβ(1−42) dimer, an Aβ(1−42) dimer based on monomeric the Aβ(1−42) peptide with enriched coil structures is constructed. The early molecular mechanisms of quercetin molecules on inhibiting the Aβ(1−42) dimer at two different Aβ42-to-quercetin molar ratios (1:5 and 1:10) are explored via all-atom molecular dynamics simulations. The results indicate that quercetin molecules can impede the configurational change of the Aβ(1−42) dimer. The interactions and the binding affinity between the Aβ(1−42) dimer and quercetin molecules in the Aβ42 dimer + 20 quercetin system are stronger in comparison with that in the Aβ42 dimer + 10 quercetin system. Our work may be helpful in developing new drug candidates for preventing the conformational transition and further aggregation of the Aβ dimer.

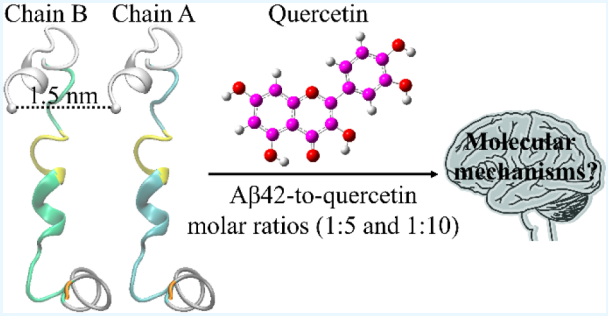

INTRODUCTION

The self-assembly and aggregation of misfolded proteins can lead to a wide range of human amyloidosis diseases such as Alzheimer's and Parkinson's diseases, type II diabetes, and amyotrophic lateral sclerosis.[1,2] Among these diseases, Alzheimer's disease (AD) is a common neurodegenerative disease, cannot be prevented or cured, and has received extensive attention in clinics. The misfolded amyloid-β (Aβ) peptide is one of the most important hallmarks for AD. Especially, Aβ consisting of 42 amino acids (Aβ42 for short) is considered to be more aggregated and neurotoxic.[3] The misfolded Aβ42 peptides can assemble into soluble oligomers and then become Aβ42 fibrils. Generally, Aβ assemblies formed during the aggregation process are toxic agents, and the Aβ dimer is identified as the smallest neurotoxic species of AD.[4,5]

The Aβ42 dimer, which is self-assembled from monomeric Aβ42 peptides, is one of the simplest oligomeric intermediates. It is reported that soluble Aβ dimers which have been extracted from brain homogenates of AD patients can perturb synapse structure and function.[5] Also, Aβ42 dimers could act as basic units for assembling and forming structures of higher order.[6,7] However, it is very challenging to study the conformational properties and transitions of Aβ42 dimers because of their transient and heterogeneous nature. Molecular dynamics (MD) simulations, which can be employed as complementary approaches to experimental studies, are utilized to give insights into the behavior processes of Aβ42 dimers without or with inhibitors on the molecular scale.[8]

MD simulations can offer information on Aβ42 dimer states and aggregation behaviors. Urbanc et al. have explored the formation of Aβ42 dimer conformation at the atomic level and predicted 10 different planar β-strand dimer conformations.[9] Zhu et al. have provided the structural properties of the three most stable dimers by performing MD simulations, indicating that the hydrophobic regions of two monomers are important in the dimerization process.[10] Furthermore, Itoh et al. have investigated the dimerization of Aβ(29−42) fragments and full-length Aβ42 peptides using the Hamiltonian replica-permutation MD simulations, illustrating that a long intermolecular β-sheet structure is reproduced, and the key residue for the Aβ42 aggregation is identified as Arg5.[11,12] The behavioral mechanisms of disrupting Aβ peptides' aggregations by ultrasonic wave and infrared laser irradiation have been

Received: February 22, 2023
Accepted: April 21, 2023
Published: May 9, 2023

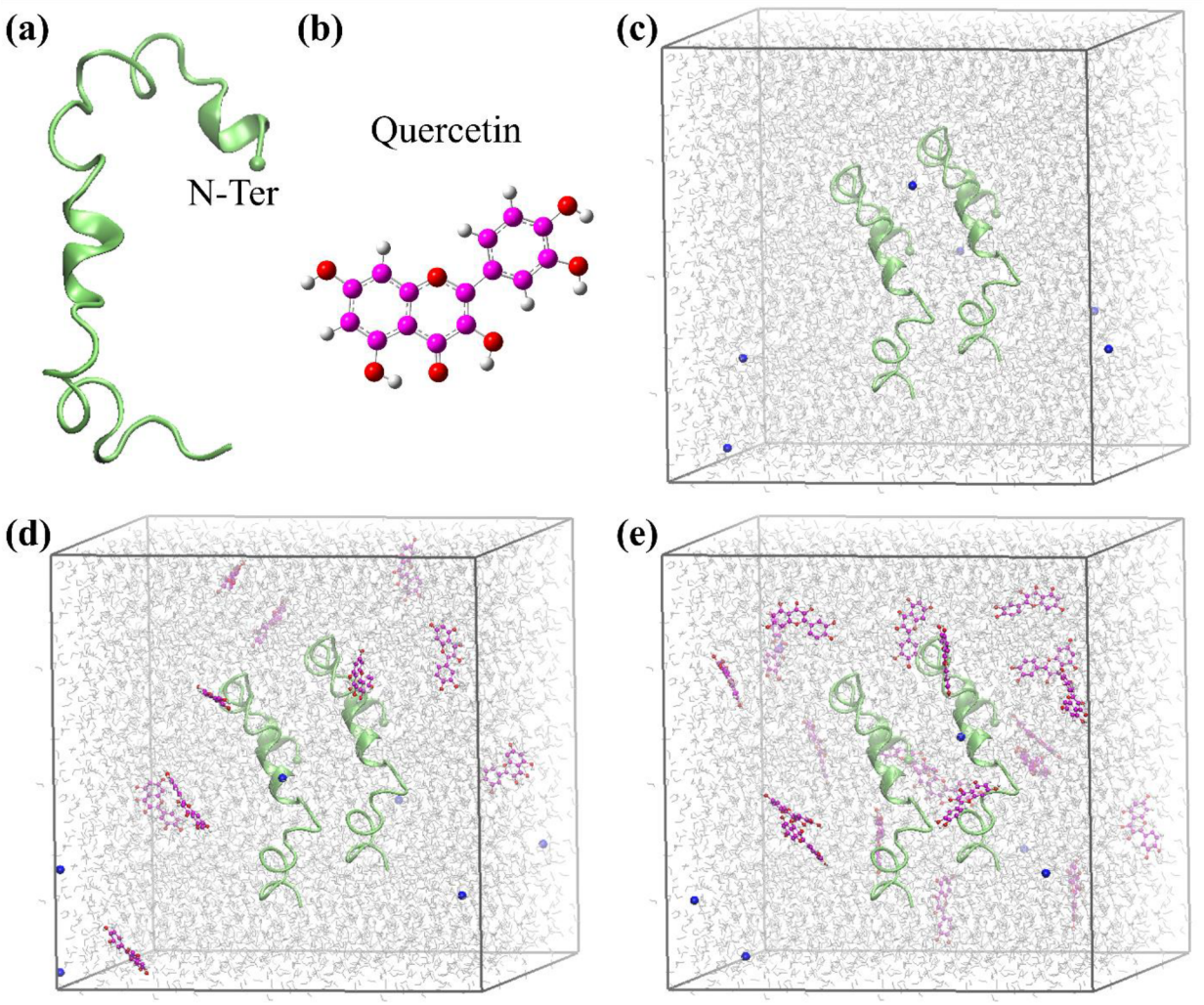

Figure 1. Structural illustration. (a) Initial structure of the Aβ42 monomer, (b) chemical structure of a quercetin molecule, (c) the initial Aβ42 dimer in water, (d) the initial Aβ42 dimer and 10 quercetin molecules in water, and (e) the initial Aβ42 dimer and 20 quercetin molecules in water. The Cα atom of the N-terminal of the Aβ42 peptide is represented by a green bead. Sodium ion as a counterion is represented by a blue bead. Water molecule is represented by a gray line.

studied using nonequilibrium MD simulations, respectively.[13,14] Moreover, Man et al. have used MD simulations to elucidate the aggregation kinetics of the Aβ42 dimer and estimate the oligomerization time for the Aβ42 dimer.[15] Chong et al. have reported the dimerization process of the Aβ42 peptides in water by using MD simulations, demonstrating that the water-induced force drives the initial nucleation stage, whereas the protein internal force drives the subsequent structural accommodation stage.[16]

On the other hand, MD simulations are adopted to investigate the interaction mechanisms between Aβ42 dimers and inhibitors. Zhao et al. have revealed the detailed interaction of the Aβ42 dimer with curcumin, suggesting that curcumin could reduce the β-sheet secondary structural content within the Aβ42 dimer.[17] Zhang et al. have investigated the inhibition effect of (−)-epigallocatechin gallate (EGCG) on the Aβ42 dimer at the molecular level, indicating that EGCG molecules are able to decrease interchain and intrachain contacts, reduce β-sheet content, and augment coil and α-helix contents of the Aβ42 dimer structures.[18] Similarly, Li et al. have performed all-atom MD simulations on Aβ42 dimers in the existence of resveratrol or EGCG molecules, implying that resveratrol molecules bind to the Aβ42 dimer mainly through $\pi-\pi$ stacking interactions, while EGCG molecules bind to the Aβ42 dimer primarily through hydrophobic, $\pi-\pi$ stacking, and hydrogen-bonding interactions.[19] Sun et al. have studied the inhibitory mechanism of 1,2-(dimethoxymethano)fullerene against Aβ42 dimer aggregation, showing that the interaction between the fullerene derivative and Aβ42 peptides significantly inhibits the formation of β-hairpins and interpeptide β-sheets in the Aβ42 dimer.[20] In addition, MD simulations have been applied to research the molecular mechanisms of norepinephrine and dopamine in inhibiting the Aβ42 dimer and have found that norepinephrine and dopamine can suppress the dimerization of Aβ42 peptides and result in disordered coil-rich Aβ42 dimers.[21,22] Computer simulations contribute to a better understanding of the Aβ42 dimer and also help to develop more effective drugs for preventing Aβ42 fibrillization.

As for potential Aβ fibrillogenesis inhibitors, natural products extracted from edible plants have attracted particular attention due to their nontoxicity and low side effects. Quercetin (3,3′,4′,5,7-pentahydroxyflavone), a common polyphenol contained in multiple fruits and vegetables, is reported

https://doi.org/10.1021/acsomega.3c01208
ACS Omega 2023, 8, 18009−18018

to exhibit the neuroprotective effects in many experimental studies.[23,24] Ansari et al. have demonstrated that quercetin can significantly attenuate Aβ42-induced oxidative cytotoxicity *in vitro*.[25] It is found that quercetin could inhibit the formation of Aβ fibrils as well as disaggregate Aβ fibrils *in vitro*.[26] Espargaro et al. have compared the anti-Aβ aggregation activity of several natural phenolic compounds by combining *in vitro* cell-based assay and *in silico* screening, showing that quercetin displays potent antiaggregation ability.[27] Moreover, quercetin is able to cross the blood−brain barrier (BBB) and shows measurable *in situ* (rat) BBB permeability.[28,29] However, the underlying inhibitory mechanism of quercetin on Aβ42 dimerization is still unknown.

Here in this study, we explore the inhibition effect of quercetin on conformational transitions of Aβ42 peptides by carrying out all-atom MD simulations. The early molecular mechanisms of two different numbers of quercetin molecules in inhibiting Aβ42 dimerization are discussed in detail. First, three different systems in the absence and presence of quercetin molecules are constructed (Figure 1). Later, we analyze the changes concerning the structures and secondary structure distributions of Aβ42 dimers influenced by quercetin molecules, the effect of quercetin molecules on hydrogen bonds of the Aβ42 dimer, and the number of contacts between quercetin and the Aβ42 dimer. Finally, the binding free energy as well as energy contribution per amino acid residue of the Aβ42 dimer in systems with two different Aβ42-to-quercetin molar ratios are calculated. Our work demonstrates that quercetin molecules can block the configurational transition of the Aβ42 dimer. The differences in the interaction mechanisms of variable amounts of quercetin molecules with the Aβ42 dimer are also addressed.

METHODS

Preparation of the System Model. The three-dimensional (3D) structure of the monomeric Aβ42 peptide is obtained from the Protein Data Bank, and the amino acid residue sequence of the Aβ42 monomer is D_1AEFRHDSGY$_{10}$EVHHQKLVFF$_{20}$AEDVGSNKGA$_{30}$IIGLMVGGVV$_{40}$IA$_{42}$. Compared to the NMR structure of the Aβ42 peptide (PDB ID: 1IYT) taken from the solvent system of the 80/20 hexafluoroisopropanol (HFIP)/water proportion which is a prevalent α-helix structure as well as the NMR structure of the Aβ42 peptide (PDB ID: 1Z0Q) derived from the solvent system of 30/70 HFIP/water proportion which is the prevalent bend structure, the 3D NMR conformation of the Aβ42 peptide (PDB ID: 6SZF) which is from the solvent system of 50/50 HFIP/water proportion is intermediate in regularity and rich in coil.[30] Therefore, model 1 of the NMR structure in PDB file 6SZF is utilized as a topology model of MD simulations (Figure 1a). The initial state of the Aβ42 dimer contains two Aβ42 peptides (labeled as chain A and chain B) which are placed in parallel with the same orientation (Figure S1). Furthermore, the distance between two monomers is 1.5 nm to build an isolated dimer system.[21] The structure of the quercetin molecule (CID: 5280343) is taken from the PubChem Database (Figure 1b). The optimization of the structure and the calculation of the electrostatic potential of the quercetin molecule is performed with the Hartree−Fock method and 6-31G(d) basis set by using Gaussian09W software.[31] Subsequently, the AmberTools package is employed to implement the electrostatic potential fit and the parametrization of the quercetin molecule.[32]

To determine the conformational behavior of the Aβ42 dimer with the presence of quercetin molecules, three system models are prepared (Figure 1c, d, and e): the Aβ42 dimer alone (Aβ42 dimer system), the Aβ42 dimer with 10 quercetin molecules (Aβ42 dimer + 10 quercetin system), and the Aβ42 dimer with 20 quercetin molecules (Aβ42 dimer + 20 quercetin system). Meanwhile, the Aβ42 dimer system is set as the control group. The Aβ42 peptide to quercetin molar ratios in the Aβ42 dimer + 10 quercetin system and the Aβ42 dimer + 20 quercetin system are 1:5 and 1:10, which are in accordance with previous experimental studies.[27,33] The quercetin molecules are randomly placed around the Aβ42 dimer which is in the center of a cubic box with 6.94 nm side length. In order to simulate the full-solvation environment, these boxes are filled with TIP3P water molecules.[34] Sodium ions, which are used as counterions, are randomly added to each system to balance the negative charges on Aβ42 peptides. The systems of the Aβ42 dimer, Aβ42 dimer + 10 quercetin, and Aβ42 dimer + 20 quercetin consist of 32511, 32414, and 32395 atoms in the respective simulation boxes.

Molecular Dynamics Simulations. All MD simulations are carried out with the GROMACS-5.1.4 software package.[35,36] The AMBER99SB-ILDN force field[37,38] is utilized to parametrize the Aβ42 dimer, which has been previously shown to estimate the secondary structure contents of the Aβ42 dimer in agreement with circular dichroism data.[39] Periodic boundary conditions are applied to the *x*, *y*, and *z* directions in the simulation boxes. The LINCS algorithm[40] is adopted to constrain the bond lengths of the Aβ42 dimer and quercetin molecules. The steepest descent algorithm is used to minimize energy for each of the systems, and then equilibration of each system is carried out using the canonical (NVT) and the isothermal−isobaric (NPT) ensembles.[41] The particle mesh Ewald (PME) method[42] is employed to calculate the electrostatic interactions with the real-space cutoff value of 1.2 nm, and the cutoff value for the van der Waals interactions is set as 1.2 nm. The V-rescale thermostat[43] and the Parrinello−Rahman barostat[44] are performed to maintain the temperature of 310 K and the pressure of 1 bar, respectively. To validate the repeatability and statistical significance, three independent MD simulations of length 300 ns for each system are run, allowing an integration time step of 0.002 ps.

Analysis Methods. The MD trajectories are analyzed through the tools of the GROMACS-5.1.4 software package, and the visual molecular dynamics (VMD) software[45] is applied to the visualization of the results. All the data presented are the average values of the results of simulating three times with different initial velocities. To monitor the structural stability of Aβ42 chains, the values of the root-mean-square deviation (RMSD), radius of gyration (Rg), root-mean-square fluctuation (RMSF), and solvent accessible surface area (SASA) are calculated. The secondary structure contents of the Aβ42 dimer are analyzed by the STRIDE algorithm[46] and the dictionary of the secondary structure of proteins (DSSP) method.[47,48] Hydrogen bonds are considered to be formed when the donor−acceptor atom distance is less than 0.35 nm, and the hydrogen-donor−acceptor atom angle is less than 30°. For the contact number between the Aβ42 dimer and quercetin, an atomic contact is defined as that formed when the distance between two heavy atoms is less than 0.54 nm (one of them has to be a carbon atom) or 0.46 nm (both are not carbon atoms). The g_mmpbsa package,[49,50] which utilizes the molecular mechanics Poisson−Boltzmann surface area

https://doi.org/10.1021/acsomega.3c01208
ACS Omega 2023, 8, 18009−18018

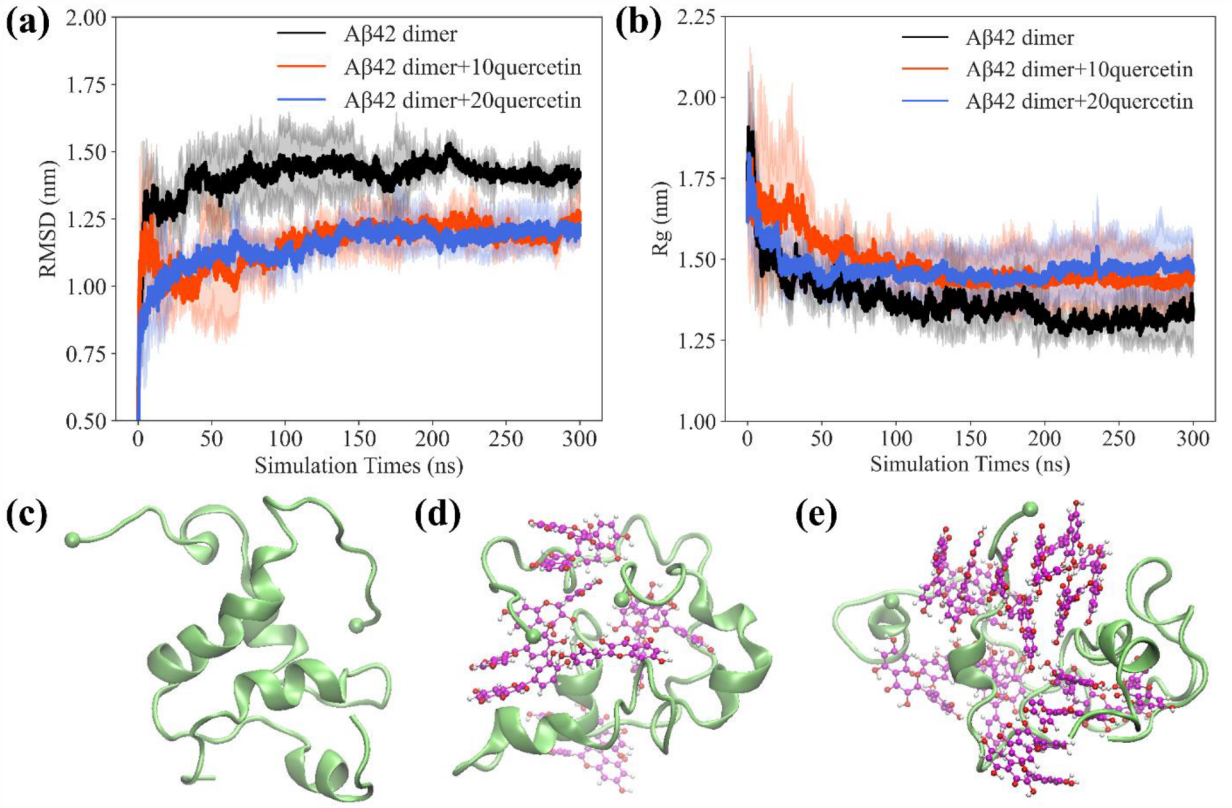

Figure 2. (a) Time evolution of backbone RMSD of the Aβ42 dimer in the absence and presence of quercetin molecules. (b) Time evolution of total Rg of the Aβ42 dimer without and with the presence of quercetin molecules. (c−e) Representative snapshots at t = 300 ns of the Aβ42 dimer in the Aβ42 dimer (c), Aβ42 dimer + 10 quercetin (d), and Aβ42 dimer + 20 quercetin (e) systems. Water molecules are not shown for clarity.

(MM-PBSA) method[51,52] for GROMACS, is adopted to calculate the binding free energy between the Aβ42 dimer and quercetin molecules, components of the binding energy, and the energetic contribution of each residue of the Aβ42 dimer to the binding of Aβ42 peptides with quercetin molecules.

RESULTS AND DISCUSSION

Structural Analysis of the Aβ42 Dimer with and without Quercetin Molecules. To estimate the conformational stability of the Aβ42 dimer in the absence and presence of quercetin molecules, the RMSD of the Aβ42 dimer's backbone atoms with respect to the energy minimized initial conformation and the time evolution of the total Rg of the Aβ42 dimer, and the RMSF and SASA values are calculated by the tools of GROMACS. As shown in Figure 2a, since the conformations of Aβ42 dimers for the three independent trajectories essentially reach the first metastable states around the initial conformations within 300 ns MD simulations, the simulation time scale of 300 ns can establish stable interactions of the Aβ42 dimer with quercetin molecules. The RMSD values of three systems attain stabilities within 100 ns, and after about 200 ns they have stabilized at approximately 1.43 ± 0.04 nm (Aβ42 dimer system), 1.21 ± 0.05 nm (Aβ42 dimer + 10 quercetin system), and 1.19 ± 0.06 nm (Aβ42 dimer + 20 quercetin system). Furthermore, the time evolution of the RMSD of each peptide chain of Aβ42 dimers with the absence and presence of quercetin molecules is shown in Figure S2a and b. The RMSD for Aβ42 dimer's chain A and chain B in three different systems is also able to achieve stability. Therefore, the 200−300 ns interval is selected to analyze the data of all results in this work.

As depicted in Figure 2b, the Rg values of three different systems show great fluctuations within 100 ns and are stabilized at about 1.31 ± 0.06 nm (Aβ42 dimer system), 1.44 ± 0.10 nm (Aβ42 dimer + 10 quercetin system), and 1.47 ± 0.09 nm (Aβ42 dimer + 20 quercetin system). The results mean that the Aβ42 dimers of three systems have experienced largely structural changes in the starting stage of the simulations, and then the structures of Aβ42 dimers remain in a stable state. The Rg values of Aβ42 dimers in the presence of quercetin molecules are larger than that of the control group, indicating that quercetin molecules are able to affect the conformational transition of the Aβ42 dimer and make the compactness of the Aβ42 dimer reduced. From Figure 2c, d, and e, compared to the control system, the conformations of Aβ42 dimers which interact with different numbers of quercetin molecules exhibit varying degrees of change after 300 ns MD simulations. More detailed analyses about the transitions of secondary structure contents of Aβ42 dimers are discussed in the section Secondary Structure Distributions of Aβ42 Dimer Influenced by Quercetin Molecules.

In addition, the average fluctuations of each amino acid residue of chain A and chain B in Aβ42 dimers are described in Figure S3a and b. Note that at Aβ42-to-quercetin molar ratios of 1:5 and 1:10 the RMSF values of most amino acid residues of chains A and B are lower than those of the control group, implying that quercetin molecules may block Aβ42 dimer deformation and reduce cytotoxicity caused by the self-assembly of Aβ42 peptides. Figure 3 displays the time

https://doi.org/10.1021/acsomega.3c01208
ACS Omega 2023, 8, 18009−18018

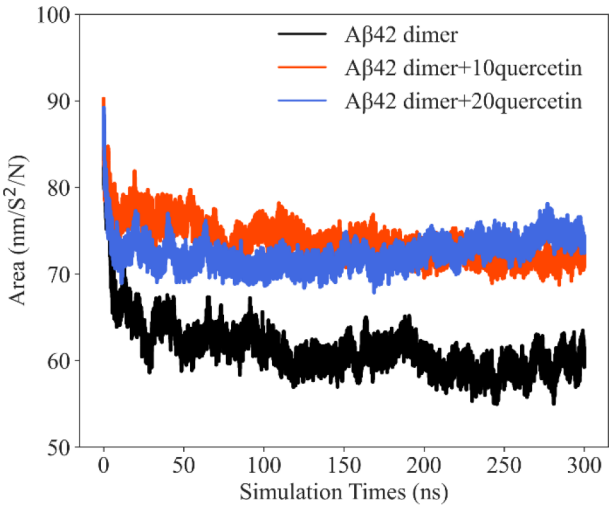

Figure 3. Time evolution of SASA values for the Aβ42 dimer in the absence and presence of quercetin molecules.

evolution of SASA values of Aβ42 dimers in three different systems. They are stable at about 59.16 ± 4.06 nm/S^2/N (Aβ42 dimer system), 72.09 ± 2.27 nm/S^2/N (Aβ42 dimer + 10 quercetin system), and 73.68 ± 6.08 nm/S^2/N (Aβ42 dimer + 20 quercetin system). Because SASA illustrates the interacting areas of the Aβ42 dimer's surface with water, the value plays an important role in affecting the conformation of a protein in water. It is obvious that the contact areas between the surfaces of the Aβ42 dimer and water molecules are significantly enlarged under the action of quercetin molecules, meaning that Aβ42 peptides are more likely to come into contact with water molecules in the presence of quercetin molecules. These results demonstrate that a large amount of quercetin molecules can hinder the configurational changes of Aβ42 peptides and prevent the self-assembly of the Aβ42 dimer.

In conclusion, the structural stability of the Aβ42 dimer in the absence or presence of quercetin molecules is investigated by combining the data of RMSD, Rg, RMSF, and SASA. The findings suggest that stable interactions between the Aβ42 dimer and quercetin molecules can be formed. Quercetin molecules may have great capabilities for stabilizing Aβ42 peptides and antiaggregating Aβ42 dimers and therefore can effectively inhibit Aβ42 fibrillization. These findings are consistent with the results reported by previous research, which has found that quercetin could block the Aβ42 polymerization progression and has inhibitory capacity in the Aβ42 aggregation.[27] Thus, quercetin molecules are able to be qualified candidates for further studying the influence of molecular action on the conformation of the Aβ42 dimer in MD simulations.

Secondary Structure Distributions of the Aβ42 Dimer Influenced by Quercetin Molecules. To explore the effect of quercetin molecules on the secondary structure distributions of the Aβ42 dimer, the secondary structure contents of the Aβ42 dimer without or with the presence of quercetin molecules are compared (Table 1). The time evolutions of the secondary structures of the Aβ42 dimer in the Aβ42 dimer system (Figure S4a), the Aβ42 dimer + 10 quercetin system (Figure S4b), and the Aβ42 dimer + 20 quercetin system (Figure S4c) are plotted. As described in Table 1 and Figure S4, the average value of random coil structures is 29.76% in the

Table 1. Comparison of Secondary Structure Contents of the Aβ42 Dimer without and with the Presence of Quercetin Molecules

secondary structure content (%)	Aβ42 dimer	Aβ42 dimer + 10 quercetin	Aβ42 dimer + 20 quercetin
coil	29.76 ± 10.26	33.44 ± 3.32	30.47 ± 5.71
β-sheet	0.51 ± 0.44	0	0
β-bridge	1.37 ± 1.22	1.77 ± 1.37	0.05 ± 0.05
bend	15.42 ± 1.60	17.26 ± 4.54	13.43 ± 0.50
turn	24.40 ± 3.49	21.20 ± 7.98	23.44 ± 4.67
helix[a]	27.36 ± 9.74	25.15 ± 1.37	31.44 ± 4.43
chain_separator	1.18 ± 0	1.18 ± 0	1.18 ± 0

[a]The α-helix, 5-helix, and 3-helix in Figure S4 correspond to the helix.

control group, while the mean contents of random coil structures are 33.44% (Aβ42 dimer + 10 quercetin system) and 30.47% (Aβ42 dimer + 20 quercetin system). The ratios of turn structures decrease from 24.40% (Aβ42 dimer system) to 21.20% (Aβ42 dimer + 10 quercetin system) and 23.44% (Aβ42 dimer + 20 quercetin system). When compared to the control system, a little increase in the average percentage of random coil structures and a slight decrease in the average value of turn structures of the Aβ42 dimer are observed in two different Aβ42-to-quercetin molar ratio (1:5 and 1:10) systems. Furthermore, as shown in Figure S4a, the intermolecular β-sheets of Aβ42 peptides can be observed after 105 ns of simulation time. It should be noted that the Aβ42 peptides are unable to form β-sheets when quercetin molecules are introduced into the Aβ42 dimer system. The average proportions of β-sheet structures of the Aβ42 dimer reduce from 0.51% in the control group to none at all in systems with quercetin molecules. In short, quercetin molecules are capable of inhibiting the formation of the β-sheet and turn structures of the Aβ42 dimer while inducing random coil structures, indicating the inhibitory effect on the conformation changes of the Aβ42 dimer.

Additionally, at Aβ42-to-quercetin molar ratio of 1:5, the average helical percentage of the Aβ42 dimer (25.15%) is less than that in the control group (27.36%), and the proportion of bend structures (17.26%) is enhanced relative to that in the control system (15.42%). However, at the Aβ42-to-quercetin molar ratio of 1:10, the average helical percentage of the Aβ42 dimer (31.44%) is more than that in the control group, and the component ratio of bend structures (13.43%) declines as compared with the control system. These results show that the binding of more quercetin molecules with the Aβ42 dimer can induce the formation of helix structures and decrease the ratio of bend structures of Aβ42 peptides. Hence, with the existence of different numbers of quercetin molecules, the varying degrees of change in the secondary structure contents of the Aβ42 dimer from β-sheet and turn structures to random coil and helix structures are identified, suggesting that the conformational conversion and further aggregation of the Aβ42 dimer can be hampered by quercetin molecules.

Effects of Quercetin Molecules on Hydrogen Bonds of the Aβ42 Dimer. To investigate the impact of quercetin molecules on hydrogen bonds of the Aβ42 dimer, the time evolution of the number of hydrogen bonds in Aβ42 dimers of the three systems is evaluated and displayed in Figure 4. Based on the data shown in Figure 4a, the mean hydrogen bond numbers within the Aβ42 dimer are about 47 ± 5 (Aβ42 dimer system), 43 ± 5 (Aβ42 dimer + 10 quercetin system), and 45

https://doi.org/10.1021/acsomega.3c01208
ACS Omega 2023, 8, 18009−18018

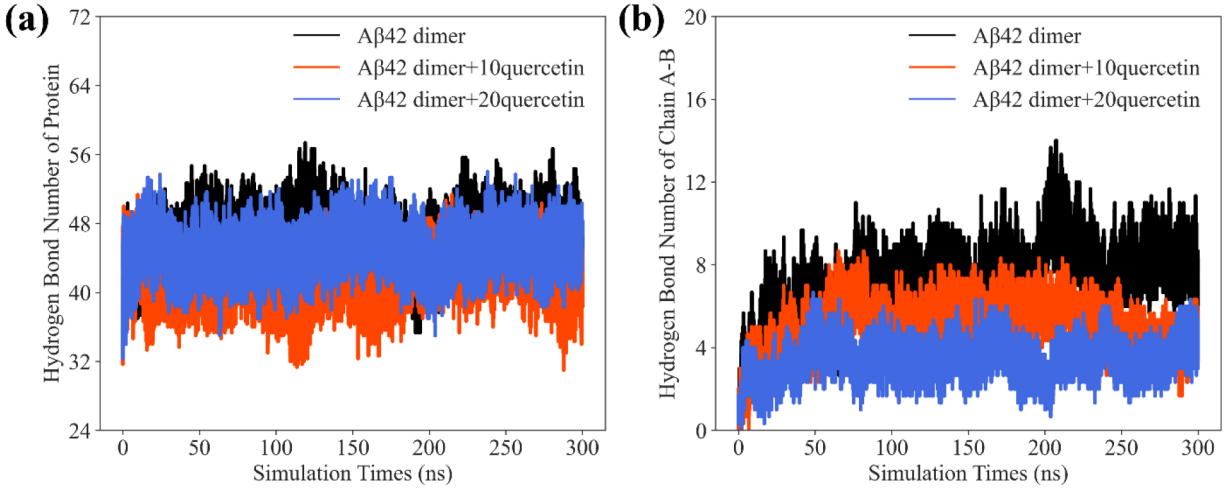

Figure 4. Effects of quercetin molecules on the hydrogen bond numbers (a) within the Aβ42 dimer and (b) between chain A and chain B of the Aβ42 dimer as a function of simulation time.

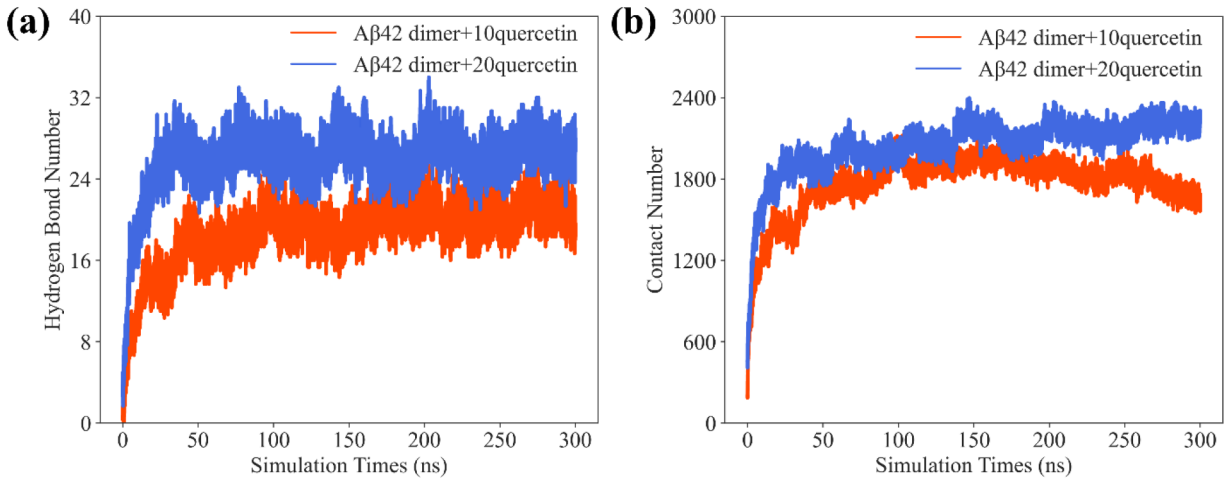

Figure 5. Hydrogen bond numbers (a) and the heavy atom contact numbers (b) between the Aβ42 dimer and quercetin molecules in the Aβ42 dimer + 10 quercetin system and the Aβ42 dimer + 20 quercetin system as a function of simulation time.

$\pm$ 8 (Aβ42 dimer + 20 quercetin system). Compared with the number of hydrogen bonds within the Aβ42 dimer in the control system, the hydrogen-bond break rates of the Aβ42 dimer are 8.51% (Aβ42 dimer + 10 quercetin system) and 4.26% (Aβ42 dimer + 20 quercetin system). Furthermore, as shown in Figure 4b, the average hydrogen bond numbers between chain A and chain B of the Aβ42 dimer in the systems of the Aβ42 dimer, Aβ42 dimer + 10 quercetin, and Aβ42 dimer + 20 quercetin are about 8 $\pm$ 4, 5 $\pm$ 4, and 4 $\pm$ 3, respectively. The number of hydrogen bonds in the Aβ42 dimer with the presence of quercetin molecules shows a slight decline in comparison with that in the Aβ42 dimer of the control group.

Moreover, the mean hydrogen bond numbers between the Aβ42 dimer and quercetin molecules maintain around 21 $\pm$ 5 (Aβ42 dimer + 10 quercetin system) and 27 $\pm$ 7 (Aβ42 dimer + 20 quercetin system), respectively (Figure 5a). It is obvious that the hydroxyl groups of quercetin molecules may possibly form stable hydrogen bonds with atoms O, N, and H of Aβ42 peptides. The results are similar to previous studies which have indicated that the hydroxyl groups of polyphenols can form hydrogen bonds with charged amino acid residues of Aβ fragments, preventing the Aβ aggregation.[53,54] Overall, our findings demonstrate that the intramolecular and intermolecular hydrogen bonds of the Aβ42 dimer are able to be partially broken by quercetin molecules. Stable hydrogen bonds between the Aβ42 dimer and polyphenol molecules are formed during the interaction process. Quercetin molecules are effective in impeding the conformational change and self-assembly of the Aβ42 dimer.

Analysis of Contact Number between the Aβ42 Dimer and Quercetin Molecules. To further investigate the interaction behavior between the Aβ42 dimer and quercetin molecules, the heavy atom contact numbers of the Aβ42 dimer with quercetin molecules in two different Aβ42-to-quercetin molar ratio systems are considered. Figure 5b shows the time evolution of the number of heavy atom contacts between the Aβ42 dimer and quercetin molecules. For the Aβ42 dimer + 10 quercetin system, the average contact numbers are kept at 1801 $\pm$ 162. Meanwhile, the mean numbers of contact are maintained at 2179 $\pm$ 268 for the Aβ42 dimer + 20 quercetin system. The results indicate that the contact numbers between the Aβ42 dimer and quercetin molecules increase markedly with the presence of a larger number of quercetin molecules. In other words, an increment of quercetin molecules can lead to more contact with Aβ42

https://doi.org/10.1021/acsomega.3c01208
ACS Omega 2023, 8, 18009−18018

peptides. The intermolecular interactions between a large amount of quercetin molecules and the Aβ42 dimer in the Aβ42 dimer + 20 quercetin system could restrict the flexibility of the Aβ42 dimer, which is in accord with the result of RMSF. Therefore, quercetin molecules are able to be responsible for stabilizing the configuration of Aβ42 peptides and inhibiting the Aβ42 dimerization process.

Analysis for Binding Free Energy between the Aβ42 Dimer and Quercetin Molecules. To monitor the interaction pattern between the Aβ42 dimer and quercetin molecules, the binding free energy is tabulated in Table 2. The

Table 2. Various Energy Terms of the Binding Free Energy between the Aβ42 Dimer and Quercetin Molecules in the Systems Aβ42 Dimer + 10 Quercetin and Aβ42 Dimer + 20 Quercetin

energy terms	Aβ42 dimer + 10 quercetin (kcal/mol)	Aβ42 dimer + 20 quercetin (kcal/mol)
ΔE_{vdW}	− 156.26 ± 14.21	−190.01 ± 14.62
ΔE_{elec}	−183.68 ± 48.95	−247.28 ± 64.16
[a]ΔE_{MM}	−339.94 ± 37.84	−437.29 ± 78.58
ΔG_{ps}	281.13 ± 47.23	376.77 ± 87.28
ΔG_{nps}	−19.55 ± 1.51	−23.73 ± 2.80
[b]ΔG_{solv}	261.59 ± 45.85	353.05 ± 84.49
[c]$\Delta G_{binding}$	−78.36 ± 9.36	−84.25 ± 10.00

[a]$\Delta E_{MM} = \Delta E_{vdW} + \Delta E_{elec}$. [b]$\Delta G_{solv} = \Delta G_{ps} + \Delta G_{nps}$. [c]$\Delta G_{binding} = \Delta E_{MM} + \Delta G_{solv}$.

collection and analysis of the last 100 ns trajectories with Δt = 100 ps in the Aβ42 dimer + 10 quercetin system and the Aβ42 dimer + 20 quercetin system are implemented. We first compare the various energy components of the binding free energy between the Aβ42 dimer and quercetin molecules. For the Aβ42 dimer + 10 quercetin system, the average value of the van der Waals interaction energy (ΔE_{vdW}) is about −156.26 ± 14.21 kcal/mol, and the mean value of the electrostatic interaction energy (ΔE_{elec}) is about −183.68 ± 48.95 kcal/mol. Yet, for the Aβ42 dimer + 20 quercetin system, the average value of ΔE_{vdW} is about −190.01 ± 14.62 kcal/mol, and the mean value of ΔE_{elec} is about −247.28 ± 64.16 kcal/mol, which suggests that the contributions of the van der Waals interactions and the electrostatic interactions heighten as the number of quercetin molecules increases.

Similar results are obtained for other energy terms. The polar contribution (ΔG_{ps}) and the nonpolar contribution (ΔG_{nps}) in the Aβ42 dimer + 10 quercetin system are about 281.13 ± 47.23 kcal/mol and −19.55 ± 1.51 kcal/mol, respectively. Also, the average value of ΔG_{ps} is about 376.77 ± 87.28 kcal/mol, and the mean value of ΔG_{nps} is about −23.73 ± 2.80 kcal/mol in the Aβ42 dimer + 20 quercetin system. Thereby, the electrostatic interactions of the Aβ42 dimer with quercetin molecules give more contribution than the van der Waals interactions to the binding affinity. Simultaneously, the polar contribution is very unfavorable for binding. The mean value of the binding free energy ($\Delta G_{binding}$ = −78.36 ± 9.36 kcal/mol) between the Aβ42 dimer and quercetin molecules in the Aβ42 dimer + 10 quercetin system is higher relative to that in the Aβ42 dimer + 20 quercetin system ($\Delta G_{binding}$ = −84.25 ± 10.00 kcal/mol). In sum, an increment of the contributions of various energy terms of the binding free energy between the Aβ42 dimer and quercetin molecules is accompanied by the presence of more quercetin molecules.

Next, we discuss the energetic contribution of the individual residue of the Aβ42 dimer to the binding between Aβ42 peptides and quercetin molecules. According to the previous study, the residues which contribute binding free energies less than −1.0 kcal/mol are considered as key residues for binding to the ligand.[55] As shown in Figure 6a, for the Aβ42 dimer + 10 quercetin system, residues F4, L17, F20, E22, D23, V24, I31, I32, M35, V36, and I41 from chain A as well as residues E3, Y10, E11, L17, F20, A21, E22, D23, V24, I31, I32, L34, M35, V36, and V39 from chain B in the Aβ42 dimer contribute lower than −1.0 kcal/mol to the binding affinity. From Figure 6b, for the Aβ42 dimer + 20 quercetin system, residues A2, E3, F4, H6, D7, S8, F20, A30, I32, V39, V40, and I41 of chain A as well as residues F4, D7, Y10, E11, L17, F19, F20, A30, I31, I32, L34, V40, and I41 of chain B in the Aβ42 dimer contribute less than −1.0 kcal/mol to the binding free energy. Nevertheless, it is worth mentioning that information on the energy contribution of each residue may be insufficient. Advanced sampling methods, such as the replica-permutation method[56] or a similar method,[57] might be used to obtain adequate statistics.

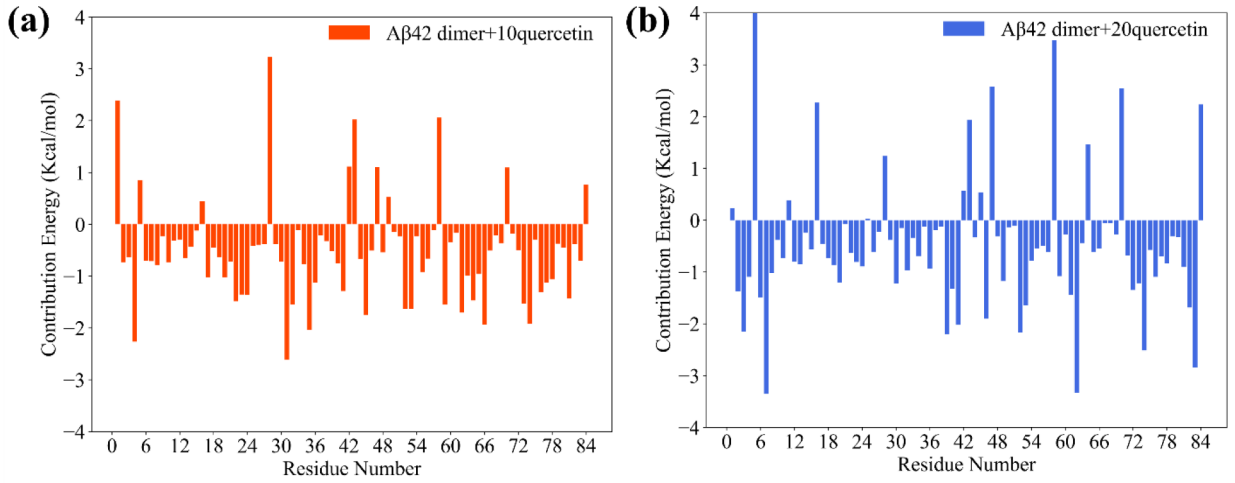

Figure 6. Contribution of individual residues of the Aβ42 dimer to the binding free energy in (a) the Aβ42 dimer + 10 quercetin system and (b) the Aβ42 dimer + 20 quercetin system.

https://doi.org/10.1021/acsomega.3c01208
ACS Omega 2023, 8, 18009−18018

The central hydrophobic core ($L_{17}VFFA_{21}$), the fragment ($I_{32}GLMVGGV_{39}$), and the C-terminus ($V_{40}IA_{42}$) of the Aβ42 peptide often serve as starting points for developing inhibitors because they are the self-recognition elements that form a β-strand.[58] Consequently, at the Aβ42-to-quercetin molar ratio of 1:5, the key residues are mainly distributed in the central hydrophobic core and the fragment, whereas at the Aβ42-to-quercetin molar ratio of 1:10, the key residues are mostly included in the N-terminus, the central hydrophobic core, and the C-terminus. There are also a small number of key residues that are involved in the fragment. The results imply that more quercetin molecules are able to strengthen the interaction with the Aβ42 dimer and show marked inhibition against the configurational change of Aβ42 peptides.

CONCLUSION

The Aβ dimer, which is the smallest neurotoxic oligomer, is able to further self-assemble into ordered fibrils leading to AD. However, due to the transient and heterogeneous nature of Aβ dimer's conformation, molecular mechanisms between the Aβ dimer and potential inhibitors cannot be well understood. Experimental studies have reported that quercetin, which is found in multiple vegetables and fruits, can block Aβ aggregation and disaggregate Aβ fibrils. Therefore, an insight into the inhibition effect of quercetin molecules on the Aβ42 dimer is the key to help in designing drug candidates for preventing Aβ fibrillization. In this work, we construct an Aβ42 dimer from the monomeric Aβ42 peptide which is rich in coil structures. The early interaction mechanisms of the Aβ42 dimer with quercetin molecules at two different Aβ42-to-quercetin molar ratios (1:5 and 1:10) are studied by all-atom MD simulations. We find that quercetin molecules are able to inhibit the conformational change of the Aβ42 dimer. Quercetin molecules could reduce the formation of β-sheet and turn structures and enhance the proportion of random coil structures of the Aβ42 dimer. Quercetin molecules at an Aβ42-to-quercetin ratio of 1:5 can hinder the self-assembly and aggregation of Aβ42 peptides, while quercetin molecules at an Aβ42-to-quercetin ratio of 1:10 exhibit stronger interactions with the Aβ42 dimer. The results show that when the number of quercetin molecules is augmented the hydrogen bond numbers, the contact numbers, and the binding affinity between the Aβ42 dimer and quercetin molecules can be increased accordingly. Our findings may aid in the development of novel drug candidates for inhibiting the structural transition of Aβ dimers.

ASSOCIATED CONTENT

Supporting Information

The Supporting Information is available free of charge at https://pubs.acs.org/doi/10.1021/acsomega.3c01208.

Initial structure of the Aβ42 dimer; time evolution of backbone RMSD of all chains of the Aβ42 dimer in the absence and presence of quercetin molecules; RMSF values for each chain of the Aβ42 dimer without and with the presence of quercetin molecules; time evolution of the secondary structure of the Aβ42 dimer in the Aβ42 dimer system, the Aβ42 dimer + 10 quercetin system, and the Aβ42 dimer + 20 quercetin system (PDF)

AUTHOR INFORMATION

Corresponding Authors

Mei Fang − *Department of Chemistry, School of Chemistry and Chemical Engineering, Northwestern Polytechnical University, Xi'an, Shaanxi 710072, China*; orcid.org/0000-0002-2754-4572; Email: fangmei@mail.nwpu.edu.cn

Ping Guan − *Department of Chemistry, School of Chemistry and Chemical Engineering, Northwestern Polytechnical University, Xi'an, Shaanxi 710072, China*; Email: guanping1113@nwpu.edu.cn

Xiaoling Hu − *Department of Chemistry, School of Chemistry and Chemical Engineering, Northwestern Polytechnical University, Xi'an, Shaanxi 710072, China*; Email: huxl@nwpu.edu.cn

Authors

Xin Wang − *Department of Chemistry, School of Chemistry and Chemical Engineering, Northwestern Polytechnical University, Xi'an, Shaanxi 710072, China*

Kehe Su − *Department of Chemistry, School of Chemistry and Chemical Engineering, Northwestern Polytechnical University, Xi'an, Shaanxi 710072, China*

Xingang Jia − *Department of Chemistry, School of Chemistry and Chemical Engineering, Northwestern Polytechnical University, Xi'an, Shaanxi 710072, China*

Complete contact information is available at: https://pubs.acs.org/10.1021/acsomega.3c01208

Notes

The authors declare no competing financial interest.

ACKNOWLEDGMENTS

This work was supported by the National Natural Science Foundation of China (No. 51433008) and the Key Research and Development Program in Shaanxi Province of China (Nos. 2022GY-198 and 2023-YBGY-295). The authors are grateful for support from the High-Performance Computing Center of Northwestern Polytechnical University.

REFERENCES

(1) Nguyen, P. H.; Ramamoorthy, A.; Sahoo, B. R.; Zheng, J.; Faller, P.; Straub, J. E.; Dominguez, L.; Shea, J. E.; Dokholyan, N. V.; De Simone, A.; et al. Amyloid oligomers: A joint experimental/computational perspective on Alzheimer's disease, Parkinson's disease, type II diabetes, and amyotrophic lateral sclerosis. *Chem. Rev.* **2021**, *121* (4), 2545−2647.

(2) Chiti, F.; Dobson, C. M. Protein misfolding, amyloid formation, and human disease: A summary of progress over the last decade. *Annu. Rev. Biochem.* **2017**, *86*, 27−68.

(3) Knopman, D. S.; Amieva, H.; Petersen, R. C.; Chetelat, G.; Holtzman, D. M.; Hyman, B. T.; Nixon, R. A.; Jones, D. T. Alzheimer disease. *Nat. Rev. Dis. Primers.* **2021**, *7* (1), 33.

(4) Klein, W. L.; Stine, W. B., Jr; Teplow, D. B. Small assemblies of unmodified amyloid beta-protein are the proximate neurotoxin in Alzheimer's disease. *Neurobiol. Aging* **2004**, *25* (5), 569−580.

(5) Shankar, G. M.; Li, S.; Mehta, T. H.; Garcia-Munoz, A.; Shepardson, N. E.; Smith, I.; Brett, F. M.; Farrell, M. A.; Rowan, M. J.; Lemere, C. A.; et al. Amyloid-beta protein dimers isolated directly from Alzheimer's brains impair synaptic plasticity and memory. *Nat. Med.* **2008**, *14* (8), 837−842.

(6) Bernstein, S. L.; Dupuis, N. F.; Lazo, N. D.; Wyttenbach, T.; Condron, M. M.; Bitan, G.; Teplow, D. B.; Shea, J. E.; Ruotolo, B. T.; Robinson, C. V.; et al. Amyloid-beta protein oligomerization and the importance of tetramers and dodecamers in the aetiology of Alzheimer's disease. *Nat. Chem.* **2009**, *1* (4), 326−331.

(7) Hayden, E. Y.; Teplow, D. B. Amyloid beta-protein oligomers and Alzheimer's disease. *Alzheimers Res. Ther.* **2013**, *5* (6), 60.
(8) Nasica-Labouze, J.; Nguyen, P. H.; Sterpone, F.; Berthoumieu, O.; Buchete, N. V.; Cote, S.; De Simone, A.; Doig, A. J.; Faller, P.; Garcia, A.; et al. Amyloid β protein and Alzheimer's disease: When computer simulations complement experimental studies. *Chem. Rev.* **2015**, *115* (9), 3518−3563.
(9) Urbanc, B.; Cruz, L.; Ding, F.; Sammond, D.; Khare, S.; Buldyrev, S. V.; Stanley, H. E.; Dokholyan, N. V. Molecular dynamics simulation of amyloid β dimer formation. *Biophys. J.* **2004**, *87* (4), 2310−2321.
(10) Zhu, X.; Bora, R. P.; Barman, A.; Singh, R.; Prabhakar, R. Dimerization of the full-length Alzheimer amyloid β-peptide (Aβ42) in explicit aqueous solution: A molecular dynamics study. *J. Phys. Chem. B* **2012**, *116* (15), 4405−4416.
(11) Itoh, S. G.; Okumura, H. Dimerization process of amyloid-beta(29−42) studied by the Hamiltonian replica-permutation molecular dynamics simulations. *J. Phys. Chem. B* **2014**, *118* (39), 11428−11436.
(12) Itoh, S. G.; Yagi-Utsumi, M.; Kato, K.; Okumura, H. Key residue for aggregation of amyloid-beta peptides. *ACS Chem. Neurosci.* **2022**, *13* (22), 3139−3151.
(13) Okumura, H.; Itoh, S. G. Amyloid fibril disruption by ultrasonic cavitation: Nonequilibrium molecular dynamics simulations. *J. Am. Chem. Soc.* **2014**, *136* (30), 10549−10552.
(14) Okumura, H.; Itoh, S. G.; Nakamura, K.; Kawasaki, T. Role of water molecules and helix structure stabilization in the laser-induced disruption of amyloid fibrils observed by nonequilibrium molecular dynamics simulations. *J. Phys. Chem. B* **2021**, *125* (19), 4964−4976.
(15) Man, V. H.; He, X.; Ji, B.; Liu, S.; Xie, X. Q.; Wang, J. Molecular mechanism and kinetics of amyloid-β42 aggregate formation: A simulation study. *ACS Chem. Neurosci.* **2019**, *10* (11), 4643−4658.
(16) Chong, S. H.; Ham, S. Atomic-level investigations on the amyloid-β dimerization process and its driving forces in water. *Phys. Chem. Chem. Phys.* **2012**, *14* (5), 1573−1575.
(17) Zhao, L. N.; Chiu, S. W.; Benoit, J.; Chew, L. Y.; Mu, Y. The effect of curcumin on the stability of Aβ dimers. *J. Phys. Chem. B* **2012**, *116* (25), 7428−7435.
(18) Zhang, T.; Zhang, J.; Derreumaux, P.; Mu, Y. Molecular mechanism of the inhibition of EGCG on the Alzheimer Aβ(1−42) dimer. *J. Phys. Chem. B* **2013**, *117* (15), 3993−4002.
(19) Li, F.; Zhan, C.; Dong, X.; Wei, G. Molecular mechanisms of resveratrol and EGCG in the inhibition of Aβ42 aggregation and disruption of Aβ42 protofibril: Similarities and differences. *Phys. Chem. Chem. Phys.* **2021**, *23* (34), 18843−18854.
(20) Sun, Y.; Qian, Z.; Wei, G. The inhibitory mechanism of a fullerene derivative against amyloid-β peptide aggregation: An atomistic simulation study. *Phys. Chem. Chem. Phys.* **2016**, *18* (18), 12582−12591.
(21) Zou, Y.; Qian, Z.; Chen, Y.; Qian, H.; Wei, G.; Zhang, Q. Norepinephrine inhibits Alzheimer's amyloid-β peptide aggregation and destabilizes amyloid-β protofibrils: A molecular dynamics simulation study. *ACS Chem. Neurosci.* **2019**, *10* (3), 1585−1594.
(22) Chen, Y.; Li, X.; Zhan, C.; Lao, Z.; Li, F.; Dong, X.; Wei, G. A comprehensive insight into the mechanisms of dopamine in disrupting Aβ protofibrils and inhibiting Aβ aggregation. *ACS Chem. Neurosci.* **2021**, *12* (21), 4007−4019.
(23) Zhang, X. W.; Chen, J. Y.; Ouyang, D.; Lu, J. H. Quercetin in animal models of Alzheimer's disease: A systematic review of preclinical studies. *Int. J. Mol. Sci.* **2020**, *21* (2), 493.
(24) Liu, R.; Zhang, T. T.; Zhou, D.; Bai, X. Y.; Zhou, W. L.; Huang, C.; Song, J. K.; Meng, F. R.; Wu, C. X.; Li, L.; et al. Quercetin protects against the Aβ(25−35)-induced amnesic injury: Involvement of inactivation of rage-mediated pathway and conservation of the NVU. *Neuropharmacology* **2013**, *67*, 419−431.
(25) Ansari, M. A.; Abdul, H. M.; Joshi, G.; Opii, W. O.; Butterfield, D. A. Protective effect of quercetin in primary neurons against Aβ(1−42): Relevance to Alzheimer's disease. *J. Nutr. Biochem.* **2009**, *20* (4), 269−275.
(26) Jimenez-Aliaga, K.; Bermejo-Bescos, P.; Benedi, J.; Martin-Aragon, S. Quercetin and rutin exhibit antiamyloidogenic and fibril-disaggregating effects in vitro and potent antioxidant activity in APPswe cells. *Life Sci.* **2011**, *89* (25−26), 939−945.
(27) Espargaro, A.; Ginex, T.; Vadell, M. D.; Busquets, M. A.; Estelrich, J.; Munoz-Torrero, D.; Luque, F. J.; Sabate, R. Combined in vitro cell-based/in silico screening of naturally occurring flavonoids and phenolic compounds as potential anti-Alzheimer drugs. *J. Nat. Prod.* **2017**, *80* (2), 278−289.
(28) Youdim, K. A.; Qaiser, M. Z.; Begley, D. J.; Rice-Evans, C. A.; Abbott, N. J. Flavonoid permeability across an in situ model of the blood-brain barrier. *Free Radic. Biol. Med.* **2004**, *36* (5), 592−604.
(29) Shimazu, R.; Anada, M.; Miyaguchi, A.; Nomi, Y.; Matsumoto, H. Evaluation of blood-brain barrier permeability of polyphenols, anthocyanins, and their metabolites. *J. Agric. Food Chem.* **2021**, *69* (39), 11676−11686.
(30) Santoro, A.; Grimaldi, M.; Buonocore, M.; Stillitano, I.; D'Ursi, A. M. Exploring the early stages of the amyloid Aβ(1−42) peptide aggregation process: An NMR study. *Pharmaceuticals* **2021**, *14* (8), 732.
(31) Frisch, M. J.; Trucks, G. W.; Schlegel, H. B.; Scuseria, G. E.; Robb, M. A.; Cheeseman, J. R.; Scalmani, G.; Barone, V.; Mennucci, B.; Petersson, G. A. et al. *Gaussian 09W, Revision A.02*; Gaussian, Inc.: Wallingford, CT, 2009.
(32) Case, D. A.; Berryman, J. T.; Betz, R. M.; Cerutti, D. S.; Cheatham, T. E., III; Darden, T. A.; Duke, R. E.; Giese, T. J.; Gohlke, H.; Goetz, A. W. et al. *AmberTools 15*; University of California: San Francisco, 2015.
(33) Regitz, C.; Dussling, L. M.; Wenzel, U. Amyloid-beta (Aβ(1−42))-induced paralysis in Caenorhabditis elegans is inhibited by the polyphenol quercetin through activation of protein degradation pathways. *Mol. Nutr. Food Res.* **2014**, *58* (10), 1931−1940.
(34) Jorgensen, W. L.; Chandrasekhar, J.; Madura, J. D.; Impey, R. W.; Klein, M. L. Comparison of simple potential functions for simulating liquid water. *J. Chem. Phys.* **1983**, *79* (2), 926−935.
(35) Hess, B.; Kutzner, C.; van der Spoel, D.; Lindahl, E. GROMACS 4: Algorithms for highly efficient, load-balanced, and scalable molecular simulation. *J. Chem. Theory Comput.* **2008**, *4* (3), 435−447.
(36) Van Der Spoel, D.; Lindahl, E.; Hess, B.; Groenhof, G.; Mark, A. E.; Berendsen, H. J. GROMACS: fast, flexible, and free. *J. Comput. Chem.* **2005**, *26* (16), 1701−1718.
(37) Hornak, V.; Abel, R.; Okur, A.; Strockbine, B.; Roitberg, A.; Simmerling, C. Comparison of multiple Amber force fields and development of improved protein backbone parameters. *Proteins: Struct., Funct., Bioinf.* **2006**, *65* (3), 712−725.
(38) Lindorff-Larsen, K.; Piana, S.; Palmo, K.; Maragakis, P.; Klepeis, J. L.; Dror, R. O.; Shaw, D. E. Improved side-chain torsion potentials for the Amber ff99SB protein force field. *Proteins: Struct., Funct., Bioinf.* **2010**, *78* (8), 1950−1958.
(39) Man, V. H.; Nguyen, P. H.; Derreumaux, P. High-resolution structures of the amyloid-β 1−42 dimers from the comparison of four atomistic force fields. *J. Phys. Chem. B* **2017**, *121* (24), 5977−5987.
(40) Hess, B.; Bekker, H.; Berendsen, H. J. C.; Fraaije, J. G. E. M.; Fraaije, J. G. LINCS: A linear constraint solver for molecular simulations. *J. Comput. Chem.* **1997**, *18* (12), 1463−1472.
(41) Melchionna, S.; Ciccotti, G.; Lee Holian, B. Hoover NPT dynamics for systems varying in shape and size. *Mol. Phys.* **1993**, *78* (3), 533−544.
(42) Darden, T.; York, D.; Pedersen, L. Particle mesh Ewald: An N·log(N) method for Ewald sums in large systems. *J. Chem. Phys.* **1993**, *98* (12), 10089−10092.
(43) Bussi, G.; Donadio, D.; Parrinello, M. Canonical sampling through velocity rescaling. *J. Chem. Phys.* **2007**, *126* (1), 014101.
(44) Nose, S.; Klein, M. L. Constant pressure molecular dynamics for molecular systems. *Mol. Phys.* **1983**, *50* (5), 1055−1076.

https://doi.org/10.1021/acsomega.3c01208
ACS Omega 2023, 8, 18009−18018

(45) Humphrey, W.; Dalke, A.; Schulten, K. VMD: Visual Molecular Dynamics. *J. Mol. Graph.* **1996**, *14* (1), 33−38.
(46) Frishman, D.; Argos, P. Knowledge-based protein secondary structure assignment. *Proteins: Struct., Funct., Genet.* **1995**, *23* (4), 566−579.
(47) Kabsch, W.; Sander, C. Dictionary of protein secondary structure: Pattern recognition of hydrogen-bonded and geometrical features. *Biopolymers* **1983**, *22* (12), 2577−2637.
(48) Hooft, R. W.; Sander, C.; Scharf, M.; Vriend, G. The PDBFINDER database: A summary of PDB, DSSP and HSSP information with added value. *Comput. Appl. Biosci.* **1996**, *12* (6), 525−529.
(49) Kumari, R.; Kumar, R.; Lynn, A. g_mmpbsa−A GROMACS tool for high-throughput MM-PBSA calculations. *J. Chem. Inf. Model.* **2014**, *54* (7), 1951−1962.
(50) Baker, N. A.; Sept, D.; Joseph, S.; Holst, M. J.; McCammon, J. A. Electrostatics of nanosystems: Application to microtubules and the ribosome. *Proc. Natl. Acad. Sci. U. S. A.* **2001**, *98* (18), 10037−10041.
(51) Luo, R.; David, L.; Gilson, M. K. Accelerated Poisson-Boltzmann calculations for static and dynamic systems. *J. Comput. Chem.* **2002**, *23* (13), 1244−1253.
(52) Homeyer, N.; Gohlke, H. Free energy calculations by the molecular mechanics Poisson-Boltzmann surface area method. *Mol. Inform.* **2012**, *31* (2), 114−122.
(53) Ngoc, L. L. N.; Itoh, S. G.; Sompornpisut, P.; Okumura, H. Replica-permutation molecular dynamics simulations of an amyloid-β(16−22) peptide and polyphenols. *Chem. Phys. Lett.* **2020**, *758*, 137913.
(54) Itoh, S. G.; Okumura, H. Promotion and inhibition of amyloid-beta peptide aggregation: Molecular dynamics studies. *Int. J. Mol. Sci.* **2021**, *22* (4), 1859.
(55) Chen, H.; Zhang, Y.; Li, L.; Han, J. G. Probing ligand-binding modes and binding mechanisms of benzoxazole-based amide inhibitors with soluble epoxide hydrolase by molecular docking and molecular dynamics simulation. *J. Phys. Chem. B* **2012**, *116* (34), 10219−10233.
(56) Itoh, S. G.; Okumura, H. Replica-permutation method with the Suwa-Todo algorithm beyond the replica-exchange method. *J. Chem. Theory Comput.* **2013**, *9* (1), 570−581.
(57) Fukuhara, D.; Itoh, S. G.; Okumura, H. Replica permutation with solute tempering for molecular dynamics simulation and its application to the dimerization of amyloid-beta fragments. *J. Chem. Phys.* **2022**, *156* (8), 084109.
(58) Doig, A. J.; Derreumaux, P. Inhibition of protein aggregation and amyloid formation by small molecules. *Curr. Opin. Struct. Biol.* **2015**, *30*, 50−56.

https://doi.org/10.1021/acsomega.3c01208
ACS Omega 2023, 8, 18009−18018